PERGAMON

Journal of Geodynamics 35 (2003) 415–423

JOURNAL OF
GEODYNAMICS

www.elsevier.com/locate/jog

Pleistocene and Recent deglaciation in Svalbard: implications for tide-gauge, GPS and VLBI measurements

J.M. Hagedoorn*, D. Wolf

GeoForschungsZentrum Potsdam, Department 1: Geodesy and Remote Sensing, Telegrafenberg, D-14473 Potsdam, Germany

Abstract

Apart from sea-level change caused by ocean-water volume change, tide-gauge measurements are also affected by vertical movement of the earth's surface and by geoid change. To study these phenomena more closely, we consider the tide-gauge station at Ny-Ålesund, Svalbard, where vertical movements are controlled by GPS and VLBI measurements. Whereas the tide-gauge record indicates a relative sea-level fall of about 2.6 mm a^{-1}, the GPS and VLBI measurements suggest a land uplift of about 5.6 mm a^{-1}. We predict the deglaciation-induced vertical movement and geoid change by combining the Pleistocene ice model ICE-3G with the newly developed Recent ice model SVAL. We find that, for particular deglaciation histories and earth models with an asthenosphere, the predicted land uplift matches the measured land uplift rather closely. However, for these combinations of ice and earth models, the predicted sea-level fall is consistently too large by at least 3 mm a^{-1}. Considering the uncertainties and simplifications involved in the study, the discrepancy weakly suggests a sea-level rise due to increased ocean-water volume.

Keywords: Glacial-isostatic adjustment; Pleistocene and recent deglaciations; Relative sea-level change

1. Introduction

One problem of determining sea-level change due to ocean-water volume change is the correction of tide-gauge measurements for vertical movement of the earth's surface and for geoid change. Newly developed methods of determining vertical movement are the analysis of GPS and VLBI measurements; the geoid change is presently monitored by the satellite mission GRACE. Without such controls, it is necessary to compute vertical movement and geoid change by means of theoretical models.

* Corresponding author.
E-mail address: jan@gfz-potsdam.de (J.M. Hagedoorn).

0264-3707/03/$ - see front matter
doi:10.1016/S0264-3707(03)00004-8

For our study, we choose Ny-Ålesund, which is located at 78.93°N and 11.87°E in Svalbard north-west of the Barents Sea. In view of its location, part of the vertical movement and geoid change measured at Ny-Ålesund is expected to be caused by the earth's viscoelastic relaxation following the Pleistocene deglaciation of Svalbard and the Barents Sea. An additional contribution results from the Recent ablation of the glaciers and ice caps in Svalbard and the earth's viscoelastic response to it. At Ny-Ålesund, tide-gauge, GPS and VLBI measurements have been taken over periods of at least 5–10 years and, therefore, sufficiently long time series for studying the problem exist.

2. Earth models, pleistocene and recent ice models

To predict the land uplift and geoid rise at Ny-Ålesund, we use a spherical, self-gravitating, viscoelastic, compressible earth model with five layers parameterized by the mass density, ρ, the Lamé constants, λ and μ, and the viscosity, η, respectively. The values of these quantities are given in Table 1. Similar earth models were used by Kaufmann and Wolf (1996) and Kaufmann and Wu (1998) for interpreting the land uplift following the Pleistocene deglaciation of Svalbard and the Barents Sea. To parameterize the Pleistocene deglaciation, we use the global ice model ICE-3G (Tushingham and Peltier, 1991). In comparison to the regional ice models BARENTS-2 (Kaufmann and Wolf, 1996) and BK-3 (Lambeck, 1996) developed for the European Arctic, ice model ICE-3G has a larger maximum thickness, a larger maximum extent and a different deglaciation history. In particular, ice models BARENTS-2 and BK-3 are limited to the Barents Sea and Novaya Zemlya. The redistribution of melt water into the oceans acts as an additional mass. Its influence on relative sea level, vertical movement and geoid change is taken into account by means of the sea-level equation (e.g. Clark et al., 1978; Mitrovica et al., 1994). For calculating the earth's response to ice model ICE3-G and the melt water redistribution, we use the global earth model MF2 (Mitrovica and Forte, 1997). It differs from that given in Table 1, but is more characteristic of the average earth. For the simulation of the Recent ablation in Svalbard, we use the newly developed regional ice model SVAL (Fig. 1). Its spatial distribution is based on the glacier atlas prepared by Hagen et al. (1993) and represents a simplified model of the actual conditions. Estimates of the mass balance of selected glaciers in Svalbard were given by Hagen and Liestøl (1990), Hagen (1995) and Dowdeswell et al. (1997). We adopt the mean value

Table 1
Parameter values used for depth to top of layer, h, mass density, ρ, Lamé constants, λ and μ, and viscosity, η[a]

h (km)	ρ (kg m^{-3})	λ (Pa)	μ (Pa)	η (Pa s)
0	3193 to 3261	1.28×10^{11}	0.57×10^{11}	∞
110	3326 to 3380	1.42×10^{11}	0.79×10^{11}	η_2
210	3712 to 3950	1.78×10^{11}	1.81×10^{11}	4.0×10^{20}
670	4458 to 5567	4.42×10^{11}	1.81×10^{11}	7.0×10^{21}
2891	10982	1.20×10^{12}	0	0

[a] The asthenosphere viscosity, η_2, is 1.0×10^{18} Pa s for earth model A1, 1.0×10^{19} Pa s for earth model A2 and 4.0×10^{20} Pa s for earth model NA.

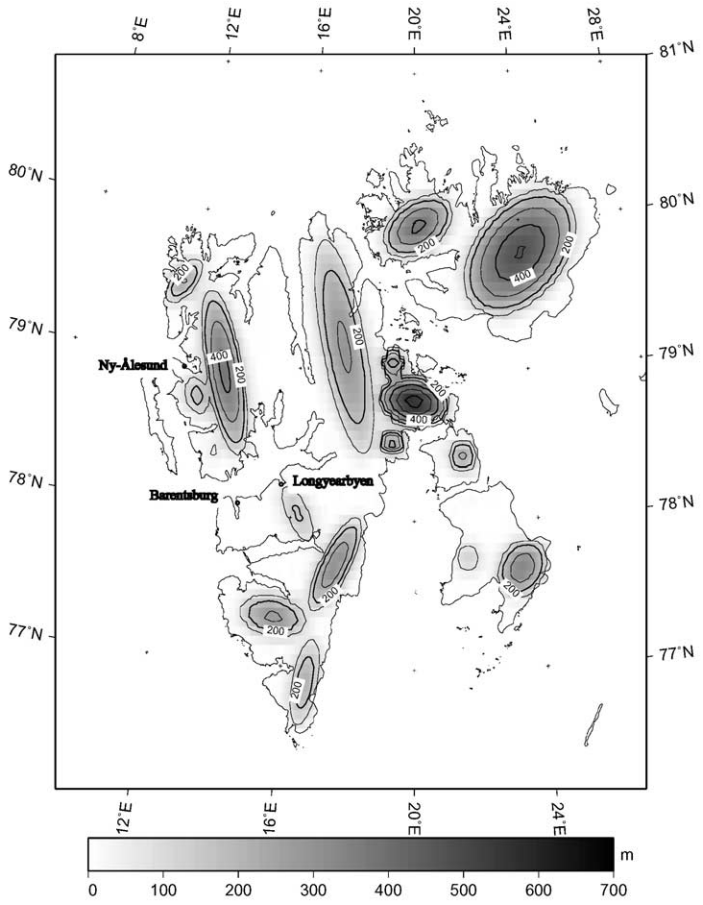

Fig. 1. Recent ice model SVAL. The isolines show the present ice thickness in units of m.

for the years 1980–1997, $b_{\mathrm{mean}} = -357$ mm a^{-1} (water equivalent). In addition, we use $b_{\mathrm{min}} = -250$ mm a^{-1} and $b_{\mathrm{max}} = -480$ mm a^{-1} to test the sensitivity of the predictions to the value adopted. The mass balance is assumed to be zero before 1900 (ice model SVAL-1) or before 1950 (ice model SVAL-2). After this, the values adopted apply uniformly over the ice-covered area shown in Fig. 1. The Recent deglaciation is connected with the Pleistocene deglaciation by assuming that a time-independent ice distribution covering the area of ice model SVAL remains from the time of deglaciation of the Barents Sea region at 11 ka B.P. for ice model ICE-3G until 1900 or 1950. We thus exclude the influence of a possible preceding accumulation phase on the predicted rates of land uplift and geoid change, which was studied by Thoma and Wolf (2001) for Iceland and Ivins and James (1999) for Patagonia.

3. Predictions of land uplift and geoid rise

The numerical computations are based on an analytical solution derived by Martinec et al. (2001) and the software developed by Thoma (2003). This allows us to predict the present rates of

land uplift, $\dot{u}$, and geoid rise, $\dot{e}$, for Ny-Ålesund. Their difference, $\dot{e} - \dot{u}$, gives the rate of relative sea-level rise, $\dot{s}$, if no change in ocean-water volume is involved at present. Thus, $\dot{s}$ does not include any contribution from a possible global sea-level rise.

The predictions listed in Tables 2 and 3 for the earth and ice models considered show a rather large variability. In particular, the influence of the asthenosphere viscosity, the ice-mass balance and the beginning of the Recent deglaciation can be seen. Changing the asthenosphere viscosity from 1.0×10^{18} Pa s (earth model A1) to 1.0×10^{19} Pa s (earth model A2) and 4.0×10^{20} Pa s (earth model NA) reduces the rates of land uplift to approximately 50% and 27%, respectively, of those applying to earth model A1. These variations are expected in view of the well-studied dependence of the uplift rates on the viscosity (e.g. Wolf et al., 1997; Ivins et al., 2002). A dependence on the

Table 2
Predicted rates of land uplift, $\dot{u}$, geoid rise, $\dot{e}$, and relative sea-level rise, $\dot{s}$, in mm a^{-1}, respectively, for ice model SVAL-1

Mass balance	Earth model		
	A1	A2	NA
$b_{\min}$	$\dot{u} = 6.29$ $\dot{e} = -0.39$ $\dot{s} = -6.68$	$\dot{u} = 3.14$ $\dot{e} = -0.50$ $\dot{s} = -3.64$	$\dot{u} = 1.72$ $\dot{e} = -0.57$ $\dot{s} = -2.29$
b_{mean}	$\dot{u} = 8.49$ $\dot{e} = -0.72$ $\dot{s} = -9.21$	$\dot{u} = 4.25$ $\dot{e} = -0.86$ $\dot{s} = -5.11$	$\dot{u} = 2.30$ $\dot{e} = -0.94$ $\dot{s} = -3.24$
$b_{\max}$	$\dot{u} = 11.23$ $\dot{e} = -1.14$ $\dot{s} = -12.37$	$\dot{u} = 5.63$ $\dot{e} = -1.31$ $\dot{s} = -6.94$	$\dot{u} = 3.02$ $\dot{e} = -1.41$ $\dot{s} = -4.43$

Table 3
Predicted rates of land uplift, $\dot{u}$, geoid rise, $\dot{e}$, and relative sea-level rise, $\dot{s}$, in mm a^{-1}, respectively, for ice model SVAL-2

Mass balance	Earth model		
	A1	A2	NA
$b_{\min}$	$\dot{u} = 5.03$ $\dot{e} = -0.43$ $\dot{s} = -5.46$	$\dot{u} = 2.60$ $\dot{e} = -0.51$ $\dot{s} = -3.11$	$\dot{u} = 1.49$ $\dot{e} = -0.58$ $\dot{s} = -2.07$
b_{mean}	$\dot{u} = 6.68$ $\dot{e} = -0.78$ $\dot{s} = -7.46$	$\dot{u} = 3.48$ $\dot{e} = -0.88$ $\dot{s} = -4.36$	$\dot{u} = 1.97$ $\dot{e} = -0.96$ $\dot{s} = -2.93$
$b_{\max}$	$\dot{u} = 8.75$ $\dot{e} = -1.21$ $\dot{s} = -9.96$	$\dot{u} = 4.57$ $\dot{e} = -1.34$ $\dot{s} = -5.91$	$\dot{u} = 2.57$ $\dot{e} = -1.43$ $\dot{s} = -4.00$

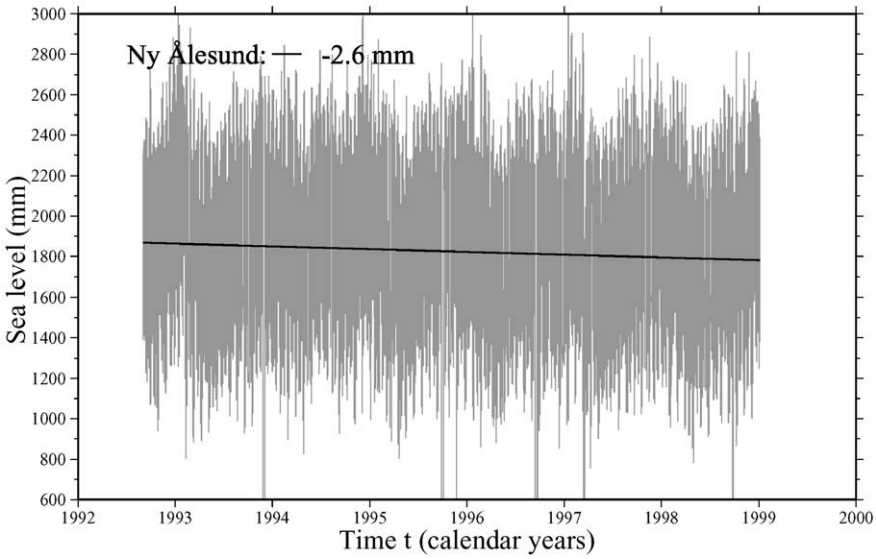

Fig. 2. Hourly tide-gauge data corrected for the inverted-barometer effect and derived linear sea-level trend.

beginning of the Recent deglaciation is also visible, where the rates of land uplift for ice model SVAL-2 (deglaciation since 1950) reach only about 80% of those for ice model SVAL-1 (deglaciation since 1900). The dependence of the predictions on the mass-balance value adopted is linear as expected.

4. Measurements of relative sea-level rise

Fig. 2 shows the tide-gauge data used for estimating the linear trend in relative sea level. The trend value is (-2.6 ± 0.7) mm a^{-1} and derived from hourly values corrected for the inverted-barometer effect on the basis of hourly air-pressure values (Braun, 1999). If monthly mean values for the period 1977–2001 provided by the PSMSL[1] are used for calculating the linear trend, a rate of (-3.1 ± 0.7) mm a^{-1} is obtained, which agrees with the trend value based on the hourly data within the uncertainties of the estimates. Since 1995, the position of Ny-Ålesund is monitored by the VLBI method. The measurements belong to campaigns involving most of Europe's VLBI stations, and the positions are referred to the centrally located VLBI station at Wettzell, Germany (Haas and Nothnagel, 1998). Accounting for the motion of Wettzell, the VLBI-derived uplift rate at Ny-Ålesund was estimated to be (5.7 ± 1.8) mm a^{-1} (Haas, 2001). Furthermore, there are two GPS stations (NALL, NYA1) of the IGS network[2] at Ny-Ålesund. The uplift rates

[1] Permanent Service for Mean Sea Level, see: http://www.pol.ac.uk/psmsl.
[2] see: http://sideshow.jpl.nasa.gov/mbh/series.html.

Table 4
Measured rates of relative sea-level rise, $\dot{s}$, and land uplift, $\dot{u}$, in mm a^{-1}, respectively, based on different methods

Method	Rate
Tide gauge	-2.6 ± 0.7
GPS (NALL)	6.30 ± 0.30
GPS (NYA1)	4.90 ± 1.54
VLBI	5.70 ± 1.80

for both stations are close to the value estimated using VLBI and are listed together with the other measurements in Table 4. The differences in the uncertainties of the GPS-derived rates reflect that NALL has been in operation since 1992, whereas NYA1 started in 1998. As uncertainties of the GPS measurements, we use twice the formal σ values given in the JPL solutions, which are based on the ITRF2000 and ellipsoidal heights in the WGS84.

5. Discussion of measurements and predictions

Inspection of the measured uplift rates (Table 4) shows that the two values based on GPS and the single value based on VLBI agree within their uncertainties. For comparing measurements

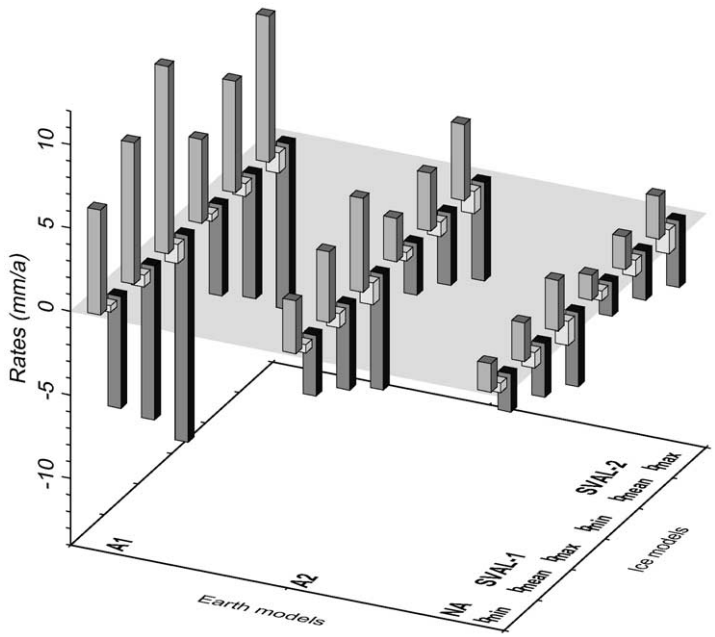

Fig. 3. Predicted rates of land uplift, $\dot{u}$, ( ), geoid rise, $\dot{e}$, ( ) and relative sea-level rise, $\dot{s}$, ( ).

and predictions, an uplift rate of (5.6±1.2) mm a^{-1} and a relative sea-level rise of (−2.6±0.7) mm a^{-1} are assumed.

As Fig. 3 shows, several combinations of earth and ice models result in predicted uplift rates near the measured uplift rate of (5.6±1.2) mm a^{-1} (e.g. ice models SVAL-1 and SVAL-2 either with b_{min} and earth model A1 or with b_{max} and earth model A2). It is thus not possible to prefer either of the mass balances, because the differences caused by earth models A1 and A2 nearly compensate their differing effects. Closer inspection of the results reveals that, for both mass-balance/earth-model combinations, the fit of the measured uplift rates produced for ice model SVAL-2 is slightly better than that for ice model SVAL-1. However, this improvement is not significant in view of the uncertainties of the measurements. The uplift rates computed using earth model NA are too small irrespective of the ice model used. This agrees with the results obtained by Kaufmann and Wolf (1996), who suggested the existence of an asthenosphere below the western part of Svalbard on the basis of their interpretation of raised post-glacial shorelines. On the other hand, for the combinations of ice and earth models permitted on the basis of the measured land uplift, we cannot reach agreement with the measured relative sea-level rise (Fig. 3). This is because the predicted rate of geoid rise is always negative and, hence, the predicted rate of relative sea-level fall is always larger than the predicted uplift rate.

The discrepancy is probably related to the assumption of presently constant ocean-water volume used in our study. In the literature, there is a wide range of estimates of the globally averaged sea-level rise, e.g. 1.1 to 1.9 mm a^{-1} (Trupin and Wahr, 1990), (1.9±0.1) mm a^{-1} (Douglas, 1997), (2.4±0.9) mm a^{-1} (Peltier and Tushingham, 1989) or (2.5±0.2) mm a^{-1} (Cabanes et al. , 2001). Obviously, these values cannot completely explain the difference of about 3 mm a^{-1} (ice model SVAL-2) or about 4 mm a^{-1} (ice model SVAL-1) between the predicted and measured rates of sea-level fall at Ny-Ålesund we obtained. However, taking into account the uncertainty of ±0.7 mm a^{-1} of the measured rate, the discrepancy is probably not overly significant. Also non-uniform changes in the sea-surface topography due to thermohaline variations are not included in our study. An additional source for the discrepancy may be the simplifications of the Recent ice model used for calculating the geoid change.

6. Summary and outlook

Combining the Pleistocene ice model ICE-3G and the newly developed Recent ice model SVAL with earth models A1 and A2 with asthenosphere allows a rather close fit of the uplift rate measured at Ny-Ålesund. However, for the combinations of ice and earth models permitted, the predicted sea-level fall is larger than the measured by at least 3 mm a^{-1}. Some of the difference may be explained by the suggested global sea-level rise. In addition, the neglect of thermohaline changes and the simplifications of the geoid calculation may be significant.

It should be helpful to include also rates of gravity change in the interpretation. So far, two campaigns with absolute gravimeters have been carried out at Ny-Ålesund, but no reliable trends are available yet. For improved predictions, it may become necessary to optimize the Pleistocene and Recent ice models with respect to spatial distribution and deglaciation history and, possibly, to take into account Recent changes of the Greenland ice sheet.

Acknowledgements

We thank E.R. Ivins and an anonymous reviewer for their constructive comments. This study was carried out within the SEAL project, German Federal Ministry of Education and Research (BMBF) Project No. SF2000/13.

References

Braun, A., 1999. Calibration of ERS altimetry data through tide gauge data in the western Spitsbergen shelf. Sci. Field Rep., LSF Grant NMA-99/2-1, 1–12.

Cabanes, C., Cazenave, A., Le Provost, Ch., 2001. Sea level rise during past 40 years determined from satellite and in situ observations. Science 294, 840–842.

Clark, J.A., Farrell, W.E., Peltier, W.R., 1978. Global change in postglacial sea level: a numerical calculation. Quat. Res. 9, 265–287.

Douglas, B.C., 1997. Global sea rise: a redetermination. Surv. Geophys. 18, 279–292.

Dowdeswell, J.A., Hagen, J.O., Björnsson, H., Glazovsky, A.F., Harrison, W.D., Holmlund, P., Jania, J., Koerner, R.M., Lefauconnier, B., Ommanney, C.S.L., Thomas, R.H., 1997. The mass balance of circum-Arctic glaciers and recent climate change. Quat. Res. 48, 1–14.

Haas, R., 2001. Personal communication. E-mail: haas@oso.chalmers.se.

Haas, R., Nothnagel, A., 1998. Crustal motion in Europe determined with geodetic Very Long Baseline Interferometry. In: Proceedings of the General Assembly of the Nordic Geodetic Commission, pp. 1–11.

Hagen, J., 1995. Recent trends in the mass balance of glaciers in Scandinavia and Svalbard. Mem. Natl. Polar Res. (Special Issue) 51, 343–354.

Hagen, J., Liestøl, D., 1990. Long-term glacier mass-balance investigation in Svalbard. Ann. Glaciol. 14, 102–106.

Hagen, J., Liestøl, D., Roland, E., Jørgensen, T., 1993. Glacier Atlas of Svalbard and Jan Mayen. Norsk Polarinstitutt, Oslo.

Ivins, E.R., James, T.S., 1999. Simple models for late Holocene and present-day Patagonia glacier fluctuations and predictions of a geodetically detectable isostatic response. Geophys. J. Int. 138, 601–624.

Ivins, E.R., Raymond, C.A., James, T.S., 2002. Late-Pleistocene, Holocene and present-day ice load evolution in the Antarctic Peninsula: models and predicted vertical crustal motion. In: Mitrovica, J.X., Vermeersen, B.L.A. (Eds.), Glacial Isostatic Adjustment, Ice Sheets, Sea Level and Dynamic Earth. American Geophysical Union, Washington DC, pp. 133–155.

Kaufmann, G., Wolf, D., 1996. Deglacial land emergence and lateral upper-mantle heterogeneity in the Svalbard Archipelago—II. Extended results for high-resolution load models. Geophys. J. Int. 127, 125–140.

Kaufmann, G., Wu, P., 1998. Lateral asthenospheric viscosity variations and postglacial rebound: a case study for the Barents Sea. Geophys. Res. Lett. 25, 1963–1966.

Lambeck, K., 1996. Limits on the areal extent of the Barents Sea ice sheet in Late Weichselian time. Global Planet. Change 12, 41–51.

Martinec, Z., Thoma, M., Wolf, D., 2001. Material versus local incompressibility and its influence on glacial-isostatic adjustment. Geophys. J. Int. 144, 136–156.

Mitrovica, J.X., Davis, J.L., Shapiro, I.I., 1994. A spectral formalism for computing three-dimensional deformations due to surface loads, 1. Theory. J. Geophys. Res. 99, 7057–7073.

Mitrovica, J.X., Forte, A.M., 1997. Radial profile of mantle viscosity: results from joint inversion of convection and postglacial adjustment. J. Geophys. Res. 102, 2751–2769.

Peltier, W.R., Tushingham, A.M., 1989. Global sea level rise and the greenhouse effect: might they be connected? Science 244, 806–810.

Thoma, M., Wolf, D., 2001. Inverting land uplift near Vatnajökull, Iceland, in terms of lithosphere thickness and viscosity stratification. In: Sideris, M.G. (Ed.), Gravity, Geoid and Geodynamics 2000. Springer-Verlag, Berlin, pp. 97–102.

Thoma, M., 2003. Materiell und lokal inkompressible viskoelastische Erdmodelle: Theorie und Anwendungen in der glazialen Isostasie. PhD thesis, University of Stuttgart, Germany.

Trupin, A., Wahr, J., 1990. Spectroscopic analysis of global tide gauge sea level data. Geophys. J. Int. 100, 441–453.

Tushingham, A.M., Peltier, W.R., 1991. Ice-3G: a new global model of late Pleistocene deglaciation based upon geophysical predictions of post-glacial relative sealevel change. J. Geophys. Res. 96, 4497–4523.

Wolf, D., Barthelmes, F., Sigmundsson, F., 1997. Predictions of deformation and gravity change caused by recent melting of the Vatnajökull ice cap, Iceland. In: Segawa, J., Fujimoto, H., Okubo, S. (Eds.), Gravity, Geoid and Marine Geodesy. Springer-Verlag, Berlin, pp. 311–319.